

## Electronic Supplementary Information

*Towards understanding photon absorption and emission in MgAl layered double hydroxide*

Bianca R. Gevers <sup>\*a</sup>, Emil Roduner <sup>b,c</sup> and Frederick J.W.J. Labuschagné<sup>a</sup>

\* Corresponding author: bianca.gevers@tuks.co.za

<sup>a</sup> Department of Chemical Engineering, Institute of Applied Materials, University of Pretoria, 0002 Pretoria, South Africa.

<sup>b</sup> Department of Chemistry, University of Pretoria, 0002 Pretoria, South Africa

<sup>c</sup> Institute of Physical Chemistry, University of Stuttgart, D-70569 Stuttgart, Germany

### Rietveld refinement

Figure S1 shows the Rietveld refinement of  $\text{Al}(\text{OH})_3$ , yielding a composition of 22.6% Gibbsite and 77.4% Bayerite. PANICSD and PDF-2 files 01-074-1775 (gibbsite) and 98-002-6830 (bayerite) were used for the fitting of the two compounds. An  $R_{wp}$  value of 7.97 was achieved.

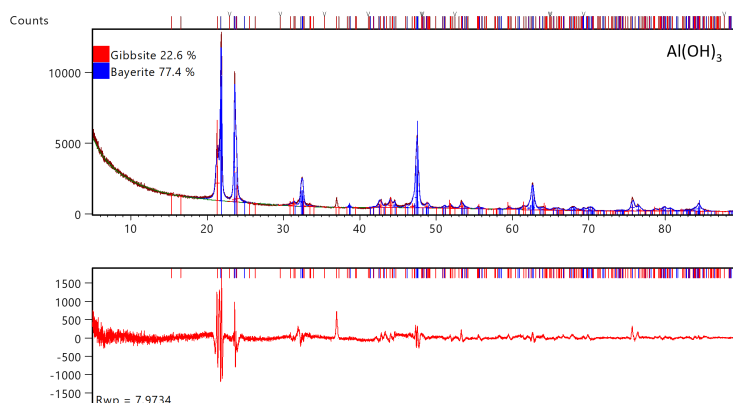


**Figure S1** Rietveld refinement of  $\text{Al}(\text{OH})_3$ .

### Bandgap determination

The bandgap of the MgAl-LDH was determined using the absorption spectrum fitting (ASF) method<sup>1</sup>. For the ASF method,  $(\text{Abs}/\lambda)^{(1/r)}$  is plotted against  $1/\lambda$ , where Abs is the absorbance,  $\lambda$  the wavelength and  $r$  the nature of the transition. LDHs are often assumed to be direct bandgap materials with allowed transitions<sup>2-5</sup>. Here the bandgap was obtained under this same assumption, thus with  $r=0.5$ . In the ASF method, a tangent line is fitted to the linear region of the spectrum and the intersection with the x-axis taken as the bandgap value<sup>1</sup>. This procedure and the resulting bandgap of 3.12 eV are shown in Figure S2. The bandgap obtained, agrees with the bandgap obtained using the alternate cut-off wavelength method.

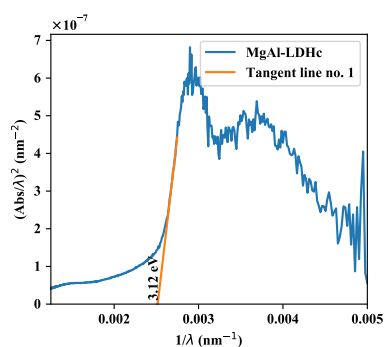


**Figure S2** Bandgap determination procedure for MgAl-LDH using the absorption spectrum fitting method.

## Deconvolution of the MIR spectrum

The MIR spectrum of MgAl-LDH was deconvoluted between  $4000\text{ cm}^{-1}$  and  $1200\text{ cm}^{-1}$  to identify the position of characteristic vibrational bands and vibrational overtones expected to be present. The region between  $4000\text{ cm}^{-1}$  and  $2000\text{ cm}^{-1}$  is shown in Figure S3 a). The region between  $2000\text{ cm}^{-1}$  and  $1200\text{ cm}^{-1}$  is shown in Figure S3 b). Both spectra were deconvoluted by making use of a baseline, 0.0019 au and 0.0035 au, respectively.

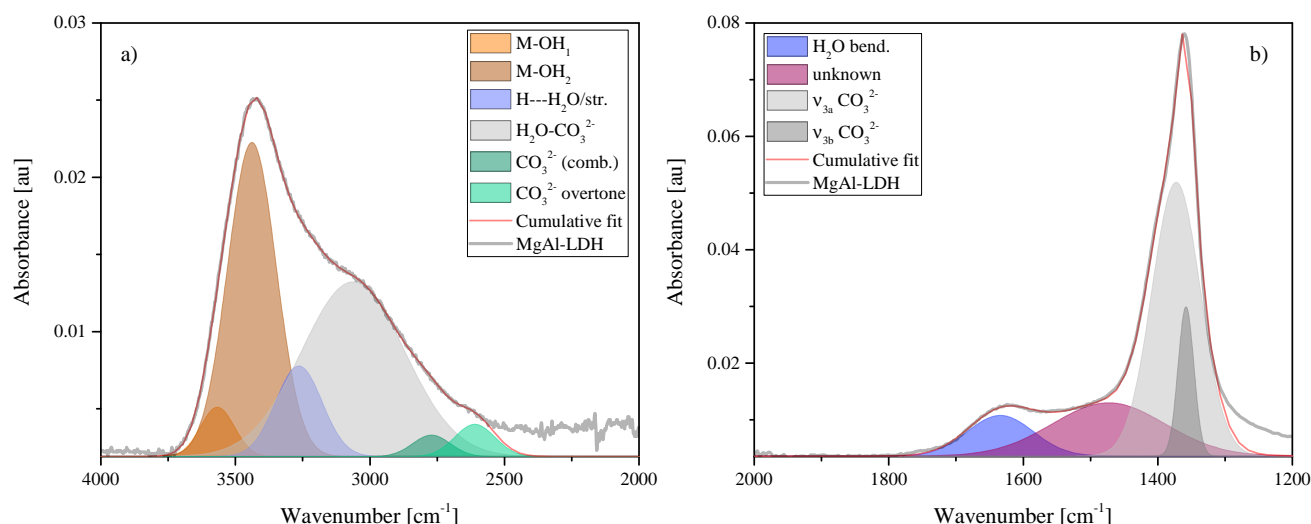


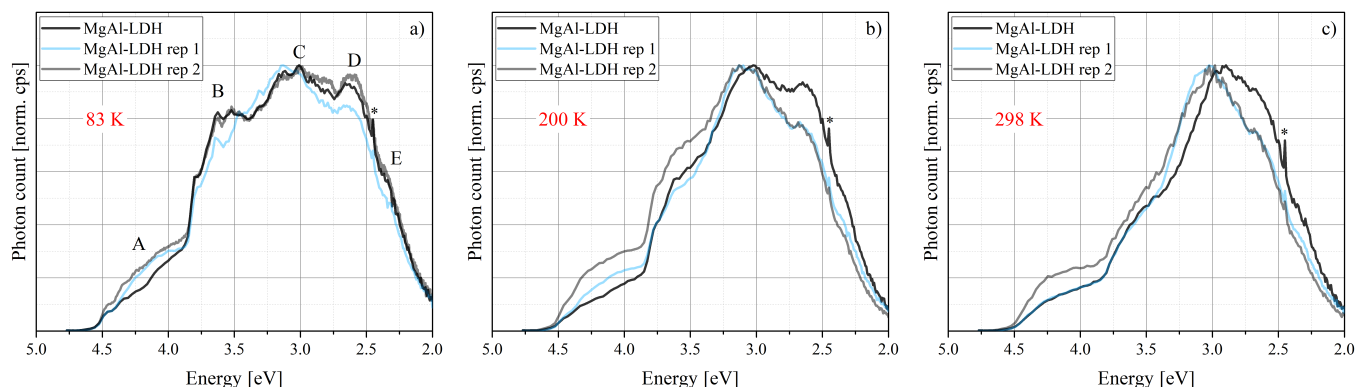
**Figure S3** a) Deconvoluted Point 11. b) Deconvoluted Peak 12 and Point 13.

## MgAl-LDH luminescence reproducibility

Figure S4 shows the reproducibility results for MgAl-LDH at 83 K, 200 K and 298 K. At 83 K, the broadest overall luminescence band with the most fine structure is observed. All luminescence spectra were recorded with a 2 nm (36.41 meV at high energy to 5.89 meV at low energy) stepsize unless stated otherwise and any resolution beyond this was lost. Some features in the spectra are considerably wider though, and part of these features thus likely represent some sort of fine structure relevant to relaxation to ground state vibrational levels. As shown in Figure S4, even small details of the PL response are reproducible at 83 K, while some differences exist at 200 K and 298 K. For these tests, three entirely different sample portions were used to test material homogeneity. At 83 K one of the materials was tested with a smaller stepsize (0.5 nm rather than 2 nm) to determine whether more fine structure could be resolved. Noise prohibited the better resolution, but the alluding multi-band, coarse-structured nature of the bands could be confirmed.

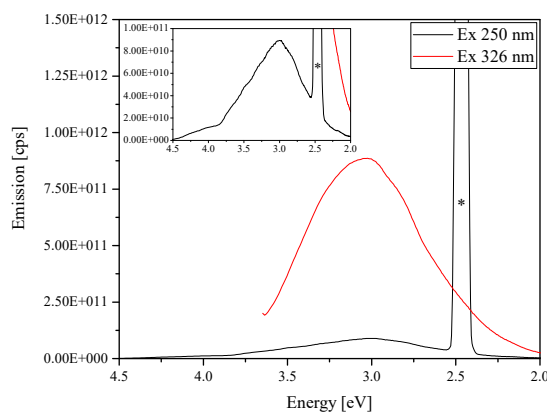
## Excitation at 250 nm and 326 nm

Figure S5 shows the luminescence spectrum obtained when exciting MgAl-LDH at 250 nm and 326 nm. The distribution of luminescence remains in both spectra remains similar but it is clearly visible, that excitation at 326 nm is much preferable to excitation at 250 nm if it is desired to increase the luminescence of MgAl-LDH. This is a result of



**Figure S4** Luminescence spectroscopy repeatability results for MgAl-LDH at a) 83 K, b) 200 K and c) 298 K. The standard stepsize was 2 nm (36.41 meV to 5.89 meV). At 83 K the luminescence of MgAl-LDH rep 2 was recorded with a stepsize of 0.5 nm (9.15 meV at 260 nm to 1.47 meV at 650 nm). \* = artefact at double excitation energy

higher absorption at the excitation wavelength but also likely of the proximity to the CB edge, thus making radiative recombination simpler.



**Figure S5** Luminescence spectrum of MgAl-LDH excited at 250 and 326 nm. \* = double excitation wavelength.

## Linear combination

Figure S6 shows the results obtained when linearly combining the hydroxide spectra in a 2Mg:1Al ratio in comparison to the spectra of MgAl-LDH at 83 K, 200 K and 298 K.

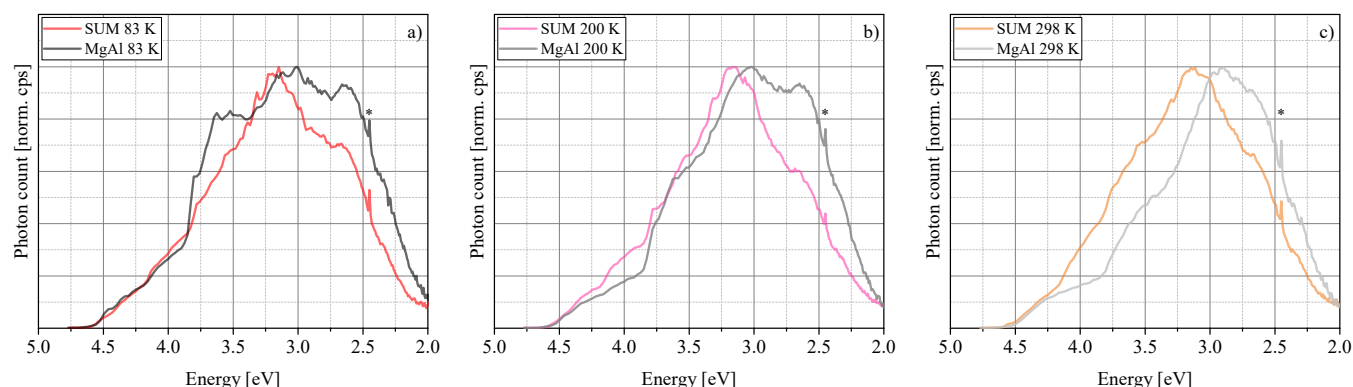


**Figure S6** Linear combination of the normalised  $\text{Mg}(\text{OH})_2$  and  $\text{Al}(\text{OH})_3$  spectra in the ratio 2Mg:1Al in comparison to the normalised MgAl-LDH spectrum. a) 83 K b) 200 K c) 298 K. \* = artefact at double excitation energy

## States

Figure S7 shows the positions of bands used to deconvolute the excitation spectra of MgAl-LDH. Hereby, the pink states depict those that there only present in some scans, resolution being lost when monitoring at lower energy

luminescence. The blue states present those present in all spectra, the yellow ones the special defect state and the green ones states below the CB edge (3.12 eV). On the right-hand side, an excerpt is shown magnifying the vibrational ground states above the VB edge.

It is important to note that the states presented here do not form a definite assignment. As a result of the deconvolution, however, they may aid as a comparative source for future research attempting to deconvolute absorption and luminescence spectra of MgAl-LDH.

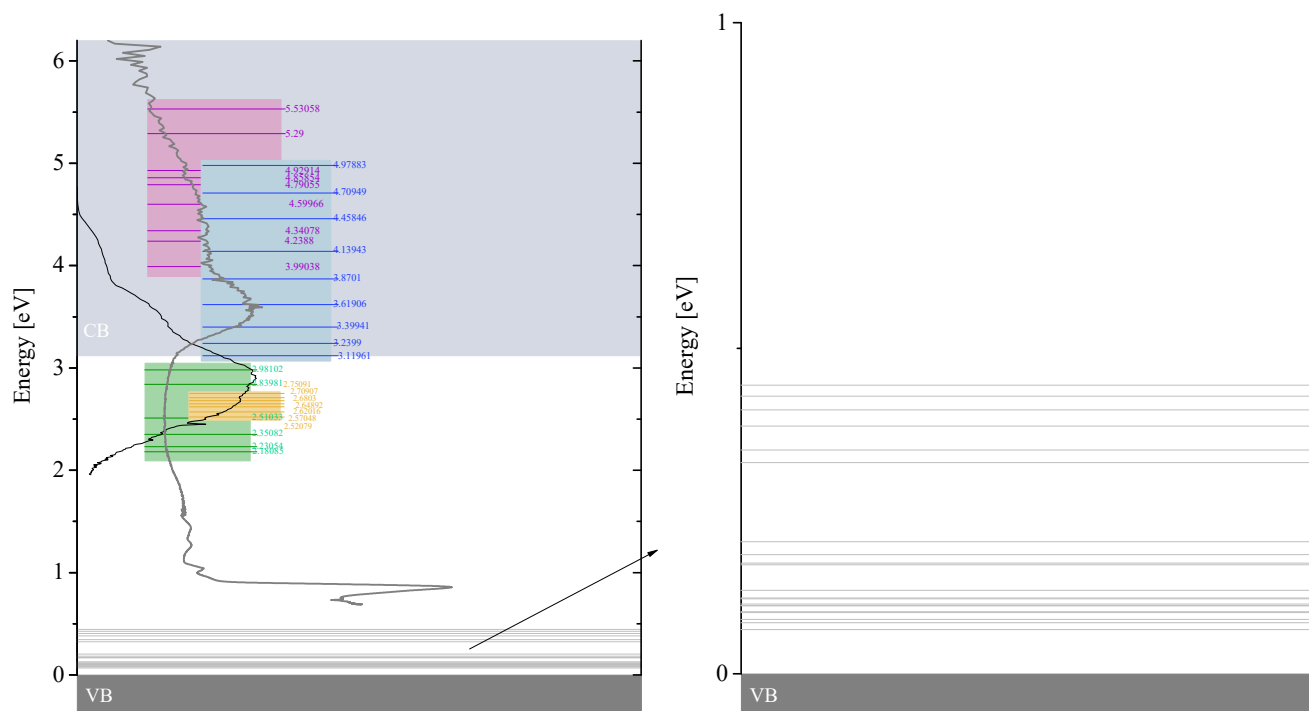


**Figure S7** States in MgAl-LDH as a result of deconvolution of the excitation spectra monitoring luminescence between 4.13 eV and 2.02 eV, and above the VB edge (vibrational ground states). These ground states are shown in magnified form on the right-hand side.

## XPS analysis

Figure S8 shows the O 1s core level of MgAl-LDH. The best fit to the experimental data was obtained by adding two Voigt line shape singlets (labelled O1 and O2 in the figure) to a Shirley-type background. The fitted components and the background are also displayed in the figure, and the overall fit shows very good agreement with the experimental data. Component O1 is located at a binding energy of 529.15 eV, while O2 is located at 530.66 eV. Based on binding energy and the relevant literature for similar compounds we can ascribe the fitted components O1 to stoichiometric oxygen ions in the main lattice matrix, while O2 to oxygen vacancies/defects in the lattice. The oxygen vacancies component O2 takes up 16% of the overall spectral weight of this core level.

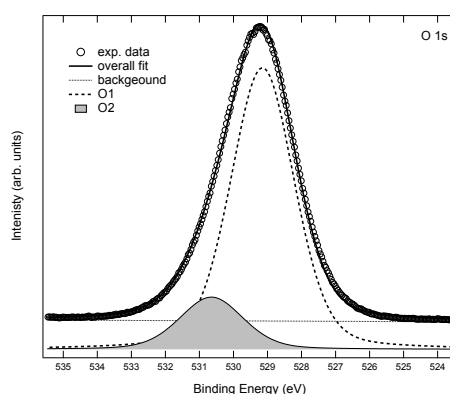


**Figure S8** XPS spectrum of MgAl-LDH.

## Calcination

Figure S9 shows luminescence spectra obtained for MgAl-LDH and MgAl-LDH calcined at 573 K and 673 K for 4 h in air acquired at 298 K.

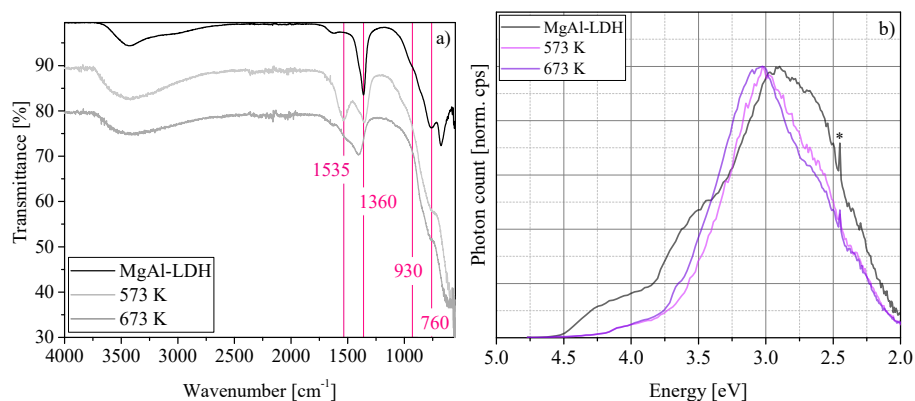


**Figure S9** a) Attenuated total reflectance Fourier-transform infrared spectra of uncalcined and calcined (at 473 K, 573 K and 673 K MgAl-LDH. b) MgAl-LDH (as is) compared to MgAl-LDH treated at 573 K and 673 K in air measured at 298 K.

## Full spectrum luminescence

Figure S10 shows full spectrum luminescence of MgAl-LDH obtained at 298 K (250 nm excitation) with a Horiba QuantaMaster 8075-22 Spectrofluorometer, slit width of 3 nm and integration time of 0.3 s. The spectrum was excitation corrected. The slight luminescence increase at 1000 nm is an experimental artefact as a result of an increase in detection sensitivity.

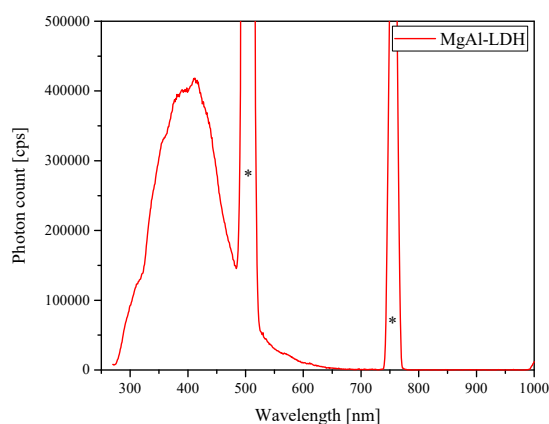


**Figure S10** Full spectrum luminescence of MgAl-LDH between 275 nm and 1000 nm (4.5 eV and 1.24 eV). \* = double and triple excitation wavelength artefacts.

## References

- [1] Ghobadi, N. Band Gap Determination Using Absorption Spectrum Fitting Procedure. *Int. Nano Lett.* **2013**, *3*, 2.
- [2] Lu, R.; Xu, X.; Chang, J.; Zhu, Y.; Xu, S.; Zhang, F. Improvement of Photocatalytic Activity of TiO<sub>2</sub> Nanoparticles on Selectively Reconstructed Layered Double Hydroxide. *Appl. Catal., B* **2012**, *111-112*, 389–396.
- [3] Zazoua, H.; Boudjemaa, A.; Chebout, R.; Bachari, K. Enhanced Photocatalytic Hydrogen Production Under Visible Light Over a Material Based on Magnesium Ferrite Derived From Layered Double Hydroxides (LDHs). *Int. J. Energ. Res.* **2014**, *38*, 2010–2018.
- [4] Dvininov, E.; Ignat, M.; Barvinschi, P.; Smithers, M.; Popovici, E. New SnO<sub>2</sub>/MgAl-Layered Double Hydroxide Composites as Photocatalysts for Cationic Dyes Bleaching. *J. Hazard. Mater.* **2010**, *177*, 150–158.
- [5] Xu, S. M.; Pan, T.; Dou, Y. B.; Yan, H.; Zhang, S. T.; Ning, F. Y.; Shi, W. Y.; Wei, M. Theoretical and Experimental Study on MIIMIII-Layered Double Hydroxides as Efficient Photocatalysts toward Oxygen Evolution from Water. *J. Phys. Chem. C* **2015**, *119*, 18823–18834.